Food Chemistry 119 (2010) 1399–1408

Contents lists available at ScienceDirect

Food Chemistry

journal homepage: www.elsevier.com/locate/foodchem

Antibacterial labdane diterpenoids of *Ulva fasciata* Delile from southwestern coast of the Indian Peninsula

Kajal Chakraborty *, A.P. Lipton [1], R. Paul Raj, K.K. Vijayan

Marine Biotechnology Division, Central Marine Fisheries Research Institute, P.B. No. 1603, Ernakulam North P.O., Cochin 682018, Kerala, India

ARTICLE INFO

Article history:
Received 29 August 2008
Received in revised form 30 July 2009
Accepted 8 September 2009

Keywords:
Ulva fasciata Delile
Ulvaceae
Antibacterial activity
Labdane diterpenoids

ABSTRACT

Chromatographic purification of the dichloromethane-soluble fraction of alga, on neutral alumina, using increasing concentrations of ethylacetate/*n*-hexane as eluents, yielded seven labdane diterpenoids (**1–7**) as major constituents of green alga *Ulva fasciata*. Structures of these diterpenoids were established using extensive spectroscopic techniques. Antimicrobial assay showed that the compounds labda-14-ene-3α,8α-diol (**2**) and labda-14-ene-8α-hydroxy-3-one (**4**) were inhibitory to the growth of *Vibrio parahaemolyticus* and *Vibrio alginolyticus* with minimum inhibitory concentrations of 30 μg/ml by **2**, and 40 μg/ml by **4**, respectively against the former and 30 μg/ml by **2**, and 80 μg/ml by **4**, respectively, against the latter. Structure–activity relationship analyses revealed that the compounds with electronegative hydroxyl or carbonyl group(s) exhibit greater activities, apparently by proton exchange reaction with the basic aminoacyl residue at the macromolecular receptor site of virulent enzymes of pathogenic bacteria. These might provide promising therapeutic agents against infections with multi-resistant Gram-negative fish pathogenic bacteria.

1. Introduction

Chlorophytan seaweeds, popularly known as green algae, are widely distributed in both inter-tidal and deep-water regions of the seas. These seaweeds are of immense pharmaceutical and agricultural value. *Ulva fasciata* Delile, a green alga (Division: Chlorophycota; Class: Ulvophyceae; Order: Ulvales), belonging to the family Ulvaceae, commonly known as "sea lettuce", grows in coastal regions of Asia–Pacific. Earlier studies have reported the antimicrobial (Selvin, Huxley, & Lipton, 2004) activities of different solvent extracts derived from this marine alga.

A wide range of compounds, particularly terpenes, polyphenolic compounds and steroids, have been reported from various marine green algae (Blunt, Copp, Munro, Northcote, & Prinsep, 2006), amongst which terpenoid compounds represent a major share. For example, *Caulerpa brownii* from Australia was reported to yield a number of bioactive novel diterpenoids and terpenoid esters (Handley & Blackman, 2005). Capisterones A and B are triterpene sulphate esters that were isolated from the tropical green alga, *Panicillus capitatus*, and were found to exhibit potent antifungal activity against the marine algal pathogen *Lindra thallasiae* (Puglisi, Tan, Jensen, & Fenical, 2004). Monocyclic diterpenes have been purified from the Tasmanian green alga *Caulerpa trifaria* (Handley & Blackman, 2000). The green alga, *Caulerpa racemosa*, was reported to yield a bioactive sesquiterpene acid (Anjaneyulu, Prakash, & Mallavadhani, 1991). Halitunal, a novel antiviral diterpene aldehyde has been isolated from the marine alga, *Halimeda tuna* (Koehn, Gunasekera, Neil, & Cross, 1991). 2-Hydroxy-1′-methylzeatin has been purified from a green alga, NIO-143, and the absolute configuration of the said cytokinin has been determined by spectroscopic procedures (Farooqi, Shukla, Shukla, & Bhakuni, 1990). Kahalalide F, a cytotoxic, antiviral and antifungal cyclic depsipeptide, was isolated from a Hawaiian species of *Bryopsis* sp. (Hamann & Scheuer, 1993). The antiinflammatory agent produced by *Ulva lactuca* was identified as 3-*O*-β-glucopyranosylstigmasta-5,25-diene (Awad, 2000). A survey of the metabolites of *U. lactuca* led to the proposal that 4-hydroxybenzoic acid is the most likely biosynthetic precursor of 2,4,6-tribromophenol, an antibacterial compound (Flodin & Whitfield, 1999). Two new antimicrobial terpenes, taxifolione and 7,7-didehydro-6-hydroxy-6,7-dihydrocaulerpenyne, were purified from *Caulerpa taxifolia*, a tropical green alga from Cap Martin, France (Guerriero et al., 1993). *Neomeris annulata*, from Kwajalein Atoll, was reported to possess three brominated sesquiterpenes, shown to deter fish feeding (Paul, Cronan Jr., & Cardellina II, 1993).

Rapid development of antibiotic resistance by many pathogens, along with the toxicity of some of the currently used antibiotics, prompts the search for, and development of novel antimicrobial

* Corresponding author. Tel.: +91 484 2394867/4069936, +91 9447084867 (mobile); fax: +91 484 2394909.
E-mail address: kajal_iari@yahoo.com (K. Chakraborty).
[1] Address: Vizhinjam Research Centre of CMFRI, P.B. No. 9, Vizhinjam P.O., Thiruvananthapuram 692521, Kerala.

0308-8146/$ - see front matter © 2009 Elsevier Ltd. All rights reserved.
doi:10.1016/j.foodchem.2009.09.019

agents from renewable sources, e.g. marine macroalgae. Marine macroalgae use targeted antimicrobial chemical defence strategies and secondary metabolites important in the ecological interactions between marine macroorganisms and microorganisms. Therefore, they could be a promising source of novel bioactive compounds. Several metabolites with unusual structures have been isolated from the green marine macroalgae, and some of these metabolites are known to exhibit high order biological activities (Blunt et al., 2006; Guerriero et al., 1993; Hamann & Scheuer, 1993). *U. fasciata* occupies a major share amongst different green algae in the coastal region of southern India. An earlier experiment in our laboratory revealed antibacterial activity of the crude methanolic extracts prepared from this green alga (Selvin et al., 2004). However, the green alga has not been exploited fully with reference to its chemical constituents and bioactive potential. In the present work, we report the bioactivity-guided isolation of seven labdane-type diterpenoid metabolites from a dichloromethane/methanol (1:1, v/v) extract of *U. fasciata*, and characterisation using spectroscopic analysis. The analyses carried out were infrared (IR), mass, and extensive nuclear magnetic resonance (^{1}H NMR and ^{13}C NMR) spectroscopic techniques, in conjunction with 2D NMR experiments. The 2D NMR techniques followed were ^{1}H–^{1}H correlation spectroscopy (^{1}H–^{1}H COSY), two-dimensional nuclear Overhauser effect correlation spectroscopy (NOESY), heteronuclear multiple quantum coherence (HMQC), and heteronuclear multiple bond coherence (HMBC). The purified compounds were evaluated for their potential antibacterial properties against marine aquacultural pathogens, namely *Vibrio parahaemolyticus* MTCC 451,*Vibrio alginolyticus* MTCC 4439, and *Vibrio vulnificus* MTCC 1145. Structure–activity relationship analyses of different classes of compounds *vis-à-vis* their antimicrobial activities can be used as a tool to elucidate the structural descriptors of a series of molecules controlling their bioactivity. In this study, we also report the structure-bioactivity correlation analyses of two series of target diterpenoids, namely labdanes and *ent*-labdanes, by utilising different electronic, hydrophobic, and steric descriptor variables to observe the variability in the substitution pattern of molecules and their effect on antibacterial activity.

2. Materials and methods

2.1. General experimental procedures

Fourier-transform infrared (FTIR) spectra of the compounds under KBr pellets were recorded in a Perkin–Elmer Series 2000 FTIR spectrophotometer. The scanning was conducted into mid IR range, i.e., between 4000 and 400 cm^{-1}. ^{1}H and ^{13}C NMR spectra were recorded on a Bruker Avance DPX 300 (300 MHz) spectrometer in $CDCl_3$ or DMSO-d_6, as aprotic solvent at ambient temperature, with TMS as internal standard. The chemical shifts (δ values) are given in parts per million (ppm) relative to TMS at 0 ppm. Standard pulse sequences were used for DEPT, ^{1}H–^{1}H COSY, two-dimensional NOESY, HMQC, and HMBC experiments. All the solvents used were either spectral grade or were distilled using glass prior to use. The GC analyses were accomplished on a Perkin–Elmer gas chromatograph equipped with an Elite-5 capillary column (30 m × 0.53 mm i.d.), using a flame ionisation detector (FID) equipped with a split/splitless injector (CAP injector), which was used in the split (1:15) mode. The oven temperature ramp programme was: 60 °C for 10 min, rising at 5 °C/min to 220 °C; injector and detector temperatures were 250 °C; carrier gas was nitrogen (ultra high purity > 99.99%, 3 ml/min). The injection port temperature was maintained at 285 °C. The injection volume was 1 μl. The GC–MS analyses were performed in electronic impact (EI) ionisation mode in a Varian GC (CP-3800) interfaced with a Varian 1200L single quadruple mass spectrometer. The GC apparatus was equipped with a WCOT fused silica capillary column of high polarity (DB-5; 30 m × 0.25 mm i.d.). The carrier gas was ultra high purity He. The injector (type 1079) and detector temperatures were maintained isothermal at 300 °C. Samples (1 μl) were injected in split (1:15) mode at 300 °C into the capillary column (similar to that used for the GC analyses) and the oven was identically programmed. Ion source and transfer line were kept at 300 °C. All chemicals were of analytical reagent grade, and were obtained from E-Merck (Darmstadt, Germany). Double-distilled and deionised water was used throughout this work. All chemical solvents used for products' isolation were of analytical grade or higher.

2.2. Algal material and preparation of algal extracts

The samples of the green alga *U. fasciata* were harvested in December 2003, from an exposed inter-tidal rocky shore in Vizhinjham and Mullur (south-west coast of India). The fresh seaweed samples were gently cleansed with filtered (0.75 μ) saline water to remove the epiphytes and other contaminants, and stored at −20 °C. The thalli of *U. fasciata* (300 g) were air-dried and milled to a fine powder. The CH_2Cl_2/CH_3OH (1:1, v/v) extract of the alga was obtained by macerating algal material for one week at room temperature. The contents were filtered and the aliquot was concentrated *in vacuo* at a temperature below 45 °C to afford a crude extract (65 g). The CH_2Cl_2/CH_3OH (1:1, v/v) extract was successively partitioned between *n*-hexane, CH_2Cl_2, and CH_3COOEt solvents. After solvent evaporation, the *n*-hexane extract furnished a viscous yellow oil (2.9 g); the CH_2Cl_2 extract gave a brown oil (12.8 g), and the CH_3COOEt extract furnished a dark brown oil (7.1 g).

2.3. Purification and structural characterisation of secondary metabolites from U. fasciata

2.3.1. General

The CH_2Cl_2 extract was fractionated by column chromatography, using neutral alumina (70–230 mesh, E-Merck, Germany) packed with *n*-hexane. The elution was initially performed using *n*-hexane containing increasing amounts of EtOAc. Simultaneously, the chromatographic procedures, e.g. thin-layer chromatography (TLC) or gas liquid chromatography (GLC), was performed to monitor the profile of various compounds in the solvent extracts. A step gradient (*n*-hexane to EtOAc; gradient ratios: 9.5:0.5, 9.0:1.0, 8.0:2.0, 7.0:3.0, 6.0:4.0, and 5.0:5.0 v/v) was followed to elute various compounds. One hundred and 88 fractions (20 ml each) were obtained after elution. The solvent fractions obtained by column chromatography were monitored on analytical TLC plates for purity, using $CHCl_3/Me_2O$ (85:15, v/v) as the solvent system. Initially, the waxy material was removed by elution, using *n*-hexane. The fractions having the same chromatograms were pooled and, finally, 11 fractions (F_1–F_{11}) were obtained. The fraction eluted with *n*-hexane/EtOAc (8:2, v/v) was repeatedly submitted to preparative TLC with *n*-hexane/EtOAc (3:1, v/v) to afford labda-14-ene-8-ol (**1**) (15.8 mg) and *ent*-labda-13(16),14-diene (**6**) (6.2 mg). From the fractions eluted with *n*-hexane/EtOAc (7:3, v/v) yellowish oily products were formed, which were further purified by alumina chromatography, using $CHCl_3/Me_2O$ (1:1, v/v) to give labda-14-ene-3α,8α-diol (**2**, 9.2 mg) and *ent*-labda-13(16),14-diene-3α-ol (**7**, 11.6 mg). The fractions eluted by *n*-hexane/EtOAc (6:4, v/v) yielded a mixture containing labda-14-ene-3α,8α-diol (**2**) and labda-14-ene-8α,9α-diol (**3**). The mixture was further subjected to normal phase neutral alumina chromatography, using increasing polarity of *n*-hexane/CH_2Cl_2, to yield pure labda-14-ene-3α,8α-diol (**2**, 1.6 mg), and labda-14-ene-8α,9α-diol (**3**, 6.1 mg). The former was eluted with *n*-hexane/CH_2Cl_2 (3:7, v/v), whilst the later was

obtained by using equivalent volumes of *n*-hexane/CH_2Cl_2 (1:1, v/v). Further TLC-guided chromatographic separations of the combined fractions F_9–F_{11} (eluted with *n*-hexane/EtOAc, 7:3, v/v) yielded twenty fractions (SF_1–SF_{20}). The eluted fractions (20 ml) were collected, and the solvents were evaporated. The fractions of similar TLC patterns were combined (SF_{10}–SF_{14}), concentrated and rechromatographed over neutral alumina columns (30 cm × 1.5 cm) with increasing polarity of *n*-hexane/EtOAc (2:8, 4:6, 6:4, and 9:1, v/v) to isolate pure labda-14-ene-8α-hydroxy-3-one (**4**, 8.2 mg) and *ent*-labda-13(16),14-diene-3-one (**5**, 9.5 mg), respectively. The fractions obtained by eluting with *n*-hexane/EtOAc (6:4, v/v) were combined, and rechromatographed on Sephadex G-20 ($CHCl_3$/EtOAc, 1:1 v/v) to afford *ent*-labda-13(16),14-diene-3α-ol (**6**, 5.8 mg). The physicochemical details of the purified compounds are as follows.

2.3.2. Labda-14-ene-8-ol (*1*)

Yellowish oil; TLC, R_f: 0.59; GC, t_R = 8.32 min; elemental analysis, found: C, 82.41; H, 5.8; O, 5.52 ($C_{20}H_{36}O$ requires C, 82.13; H, 12.40; O, 5.47); UV (CH_3OH), λ_{max} (log ε) 225 (3.11); IR cm^{-1}, ν_{max} (KBr): 3415 (OH), 2908, 2846 (methyl CH str.), 1740, 1670, 1615, 1452, 1389, 1275, 1026, 940; ^1H ($CDCl_3$, 300 MHz, δ ppm) and ^{13}C NMR ($CDCl_3$, δ ppm) (Table 1); EIMS, *m*/*z* (% rel. int.) 292 ($[M]^+$, 4), 246 (14), 264 (18), 220 (10), 208 (16), 180 (13), 166 (*100*), 122 (14), 70 (81), 82 (38), 58 (86).

2.3.3. Labda-14-ene-3α,8α-diol (*2*)

Colourless gum; TLC, R_f: 0.41; GC, t_R = 10.76 min; elemental analysis, found: C, 80.11; H, 11.83; O, 10.92 ($C_{20}H_{36}O_2$ requires C, 77.87; H, 11.76; O, 10.37); UV (CH_3OH), λ_{max} (log ε) 225 (2.88), 315 (2.96) nm; IR cm^{-1}, ν_{max} (KBr): 3450 (OH), 1260 (C–O), 3300 (as. sec. OH str.), 2957 (methyl CH str.), 2830 (methyl CH str.), 1660, 1530 (C–O), 1253, 920 (olefinic moiety); ^1H ($CDCl_3$, 300 MHz, δ ppm) and ^{13}C NMR ($CDCl_3$, δ ppm) (Table 1); EIMS, *m*/*z* (% rel. int.) 308 ($[M]^+$, 9), 308 (19), 264 (79), 220 (43), 208 (29), 180 (26), 166 (*100*), 122 (26), 175 (30), 140 (12), 98 (82), 96 (73), 58 (42).

2.3.4. Labda-14-ene-8α,9α-diol (*3*)

Pale yellow oil; TLC, R_f: 0.48; GC, t_R = 9.16 min; elemental analysis, found: C, 78.06; H, 12.39; O, 10.41 ($C_{20}H_{36}O_2$ requires C, 77.87; H, 11.76; O, 10.37); UV (CH_3OH), λ_{max} (log ε) 227 nm (2.86); IR cm^{-1}, ν_{max} (KBr): 3550 (OH), 3329 (as. sec. OH str.), 2896 (methyl CH str.), 1529, 1278 cm^{-1} (C–O); ^1H ($CDCl_3$, 300 MHz, δ ppm) and ^{13}C NMR ($CDCl_3$, δ ppm) (Table 2); EIMS, *m*/*z* (% rel. int.) 308 ($[M]^+$, 4); 264 (23), 208 (59), 220 (73), 166 (*100*), 98 (92), 82 (76).

2.3.5. Labda-14-ene-8α-hydroxy-3-one (*4*)

Colourless oil; TLC, R_f: 0.41; GC, t_R = 12.18 min; elemental analysis, found: C, 78.62; H, 11.26; O, 10.50 ($C_{20}H_{34}O_2$ requires C, 78.38; H, 11.18; O, 10.44); UV (CH_3OH), λ_{max} (log ε) 225 (2.88), 315 (2.96) nm; IR cm^{-1}, ν_{max} (KBr): 3562 (OH), 1265 cm^{-1} (C–O), 1705 cm^{-1} (C=O), 3300 (as. O= str.), 1715 (C=O ester str.), 1682 (amide-I band, C=O str.); ^1H ($CDCl_3$, 300 MHz, δ ppm) and ^{13}C NMR ($CDCl_3$, δ ppm) (Table 2); EIMS, *m*/*z* (% rel. int.) 306 ($[M]^+$, 18), 264 (41), 209 (20), 221 (56), 181 (69), 166 (100), 172 (97), 161 (14), 154 (96), 136 (36), 121 (74), 111 (65), 98 (91), 91 (38), 71 (95), 43 (*100*), 140 (22), 96 (69), 58 (53).

Table 1
^1H NMR and ^{13}C NMR spectral data of compounds **1** and **2** (300 MHz, $CDCl_3$, DMSO-d_6, δ values)[a]; the δ values are in ppm.

C. No.	Compound **1**					Compound **2**				
	δ ^{13}C NMR[b]	H	δ ^1H NMR	H–H-COSY	HMBC (H–C)	δ ^{13}C NMR[b]	H	δ ^1H NMR	H–H-COSY	HMBC (H–C)
1	38.1 (CH_2)	1a	1.43 (1H, *m*)	H-2	–	34.0 (CH_2)	1a	1.53 (1H, *m*)	H-2	–
		1b	1.56 (1H, *t*, *J* = 6.5 Hz)	–	–		1b	1.62 (1H, *t*, *J* = 6.2 Hz)	–	–
2	18.3 (CH_2)	2a	1.46 (1H, *m*)	H-1	–	26.6 (CH_2)	2a	1.76 (1H, *m*)	H-1	C-3, 4
		2b	1.59 (1H, *m*)	–	–		2b	1.89 (1H, *dd*, J_1 = 1.6 Hz; J_2 = 2.4 Hz)	–	–
3	43.4 (CH_2)	3a	1.18 (1H, *t*, *J* = 7.4 Hz)	–	–	78.5 (CH)	3	3.27 (1H, *t*, *J* = 6.4 Hz)	–	C-5, 6
		3b	1.30 (1H, *t*, *J* = 13.2 Hz)	–	–		3-OH	2.28 (*bs*)	–	–
4	32.5 (C)			–	–	39.4 (C)			–	–
5	59.9 (CH)	5	1.67 (1H, *m*)	H-5	C-4, 6,10,18,19	50.2 (CH)	5	1.69 (1H, *t*, *J* = 10.6 Hz)	H-5	C-4, 6,10,18,19
6	15.2 (CH_2)	6a	1.49 (1H, *m*)	H-6	C-8, 10, 11	14.9 (CH_2)	6a	1.40 (1H, *m*)	H-6	C-8, 10,11
		6b	1.63 (1H, *d*, *J* = 2.4 Hz)	–	–		6b	1.59 (1H, *d*, *J* = 1.8 Hz)	–	–
7	40.7 (CH_2)	7a	1.39 (1H, *m*)	–	C-8	38.6 (CH_2)	7a	1.50 (1H, *d*, *J* = 2.1 Hz)	–	C-8
		7b	1.50 (1H, *m*)	–	–		7b	1.56 (1H, *dd*, J_1 = 3.6 Hz; J_2 = 11.5 Hz)	–	–
8	73.9 (C)	8-OH	2.20 (*bs*)	–	C-8, 11	71.5 (C)	8-OH	2.18 (*bs*)	–	C-8, 11
9	59.8 (CH)	9	1.52 (1H, *dd*, J_1 = 2.1 Hz; J_2 = 6.2 Hz)	–	–	56.8 (CH)	9	1.65 (1H, *m*)	–	–
10	33.8 (C)			–	–	32.2 (C)			–	–
11	19.4 (CH_2)	11a	1.28 (1H, *m*)	–	C-9, 10,12	17.3 (CH_2)	11a	1.29 (1H, *m*)	–	C-9, 10,12
		11b	1.33 (1H, *t*, *J* = 12.8 Hz)				11b	1.35 (1H, *t*, *J* = 12.1 Hz)		
12	36.4 (CH_2)	12a	1.14 (1H, *d*, *J* = 6.6 Hz)	–	C-10, 11,12	35.6 (CH_2)	12a	1.22 (1H, *d*, *J* = 5.2 Hz)	–	C-10, 11,12
		12b	1.25 (1H, *t*, *J* = 13.2 Hz)				12b	1.31 (1H, *t*, *J* = 10.6 Hz)		–
13	40.2 (CH)	13	2.31 (1H, *m*)	–	–	41.8 (CH)	13	2.34 (1H, *m*)	–	–
14	136.4 (CH)	14	5.68 (1H, *dd*, J_1 = 5.4 Hz; J_2 = 9.2 Hz)	–	C-7, 8,12	139.2 (CH)	14	5.75 (1H, *m*)	–	C-7, 8
15	114.8 (CH_2)	15a	4.92 (1H, *t*, *J* = 1.5 Hz)	–	C-12, 13,14	118.6 (CH_2)	15a	5.03 (1H, *t*, *J* = 6.5 Hz)	–	C-12, 13,14
		15b	5.10 (1H, *m*)	–	–		15b	5.19 (1H, *m*)	–	–
16	20.6 (CH_3)	CH_3-16	1.09 (3H, *s*)	–	–	25.8 (CH_3)	CH_3-16	1.18 (3H, *s*)	–	–
17	26.3 (CH_3)	CH_3-17	1.37 (3H, *s*)	–	C-7, 9	28.0 (CH_3)	CH_3-17	1.37 (3H, *s*)	–	C-7, 9
18	26.1 (CH_3)	CH_3-18	0.93 (3H, *s*)	–	C-3, 4,5,19	18.1 (CH_3)	CH_3-18	1.06 (3H, *s*)	–	C-3, 4,5,19
19	26.5 (CH_3)	CH_3-19	0.98 (3H, *s*)	–	C-3, 4,5,18	18.9 (CH_3)	CH_3-19	1.10 (3H, *s*)	–	C-3, 4,5,18
20	20.8 (CH_3)	CH_3-20	1.19 (3H, *s*)	–	C-1, 5,9,10	23.4 (CH_3)	CH_3-20	1.23 (3H, *s*)	–	C-1, 5,9,10

C. No. signifies carbon number; [a]NMR spectra recorded using Bruker DPX 300 and AVANCE 300 MHz spectrometers, values in ppm, multiplicity and coupling constants (Hz) in parentheses; [b]the ^{13}C NMR data are validated with the DEPT experiments. The complete structural assignments were made with the aid of ^1H–^1H COSY, HMBC, and HSQC spectra.

Table 2
^{1}H NMR and ^{13}C NMR spectral data of compounds **3** and **4** (300 MHz, $CDCl_3$, DMSO-d_6, δ values)[a]; the δ values are in ppm.

C. No.	Compound **3**					Compound **4**				
	δ ^{13}C NMR[b]	H	δ ^{1}H NMR	H–H-COSY	HMBC(H–C)	δ ^{13}C NMR[b]	H	δ ^{1}H NMR	H–H-COSY	HMBC(H–C)
1	31.5 (CH_2)	1a	1.45 (1H, *m*)	H-2	–	40.2 (CH_2)	1a	1.82 (1H, *m*)	H-2	C-10
		1b	1.58 (1H, *t*, *J* = 9.3 Hz)	–	–		1b	1.91 (1H, *m*)	–	–
2	20.3 (CH_2)	2a	1.50 (1H, *m*)	–	C-3, 5	33.9 (CH_2)	2a	2.24 (1H, *m*)	H-1	C-3, 4
		2b	1.62 (1H, *m*)		–		2b	2.33 (1H, *t*, *J* = 5.2 Hz)	–	–
3	40.9 (CH_2)	3a	1.16 (1H, *t*, *J* = 12.1 Hz)	H-4	C-4, 6	221.4 (C)	–	–	–	–
		3b	1.29 (1H, *t*, *J* = 6.6 Hz)	–	–		–	–	–	–
4	33.6 (C)			–	–	48.6 (C)	–	–	–	–
5	58.4 (CH)	5	1.54 (1H, *m*)	H-5	C-4, 6,10,18,19	51.7 (CH)	5	1.71 (1H, *t*, *J* = 10.6 Hz)	H-5	C-4, 6,10,18,19
6	16.8 (CH_2)	6a	1.37 (1H, *m*)	H-6	C-8, 10,11	15.1 (CH_2)	6a	2.12 (1H, *m*)	H-6	C-8, 10,11
		6b	1.65 (1H, *d*, *J* = 2.6 Hz)	–			6b	2.17 (1H, *d*, *J* = 6.5 Hz)		–
7	35.6 (CH_2)	7a	1.41 (1H, *m*)	H-8	C-8	38.9 (CH_2)	7a	1.48 (1H, *d*, *J* = 1.8 Hz)	H-8	C-8
		7b	1.70 (1H, *m*)	–	–		7b	1.67 (1H, *dd*, J_1 = 6.5 Hz; J_2 = 2.8 Hz)		–
8	86.9 (C)	8-OH	2.09 (*bs*)	–	C-8, 11	76.8 (C)	8-OH	2.39 (*bs*)	H-7	C-8, 11
9	92.4 (CH)	9-OH	2.15 (*bs*)	–	–	55.3 (CH)	9	1.54 (1H, *m*)	–	–
10	36.7 (C)			–	–	32.1 (C)			–	–
11	25.3 (CH_2)	11a	1.47 (1H, *t*, *J* = 5.8 Hz)	H-12	C-9, 10,12	19.6 (CH_2)	11a	1.30 (1H, *m*)	H-12	C-9, 10,12
		11b	1.76 (1H, *d*, *J* = 9.3 Hz)	–	–		11b	1.37 (1H, *t*, *J* = 9.3 Hz)	–	–
12	29.4 (CH_2)	12a	1.19 (1H, *d*, *J* = 6.6 Hz)	H-11	C-10, 11,12	37.6 (CH_2)	12a	1.20 (1H, *d*, *J* = 7.4 Hz)	H-11	C-10, 11,12
		12b	1.32 (1H, *t*, *J* = 11.2 Hz)	–	–		12b	1.26 (1H, *t*, *J* = 5.8 Hz)	–	–
13	38.7 (CH)	13	2.39 (1H, *m*)	–	–	41.6 (CH)	13	2.29 (1H, *m*)	–	–
14	137.5 (CH)	14	5.82 (1H, *m*)	–	C-7, 8,12	138.2 (CH)	14	5.78 (1H, *m*)	–	C-7, 8
15	118.4 (CH_2)	15a	4.90 (1H, *t*, *J* = 6.6 Hz)	–	C-12, 13,14	116.4 (CH_2)	15a	5.11 (1H, *t*, *J* = 6.6 Hz)	–	C-12, 13,14
		15b	4.98 (1H, *m*)	–	–		15b	5.25 (1H, *m*)	–	–
16	22.4 (CH_3)	CH_3-16	1.24 (3H, *s*)	–	–	24.5 (CH_3)	CH_3-16	1.16 (3H, *s*)	–	–
17	18.8 (CH_3)	CH_3-17	1.68 (3H, *s*)	–	C-7, 9	26.9 (CH_3)	CH_3-17	1.35 (3H, *s*)	–	C-7, 9
18	26.3 (CH_3)	CH_3-18	1.08 (3H, *s*)	–	C-3, 4,5,19	23.3 (CH_3)	CH_3-18	1.09 (3H, *s*)	–	C-3, 4,5,19
19	27.4 (CH_3)	CH_3-19	1.13 (3H, *s*)	–	C-3, 4,5,18	25.6 (CH_3)	CH_3-19	1.14 (3H, *s*)	–	C-3, 4,5,18
20	16.3 (CH_3)	CH_3-20	1.21 (3H, *s*)	–	C-1, 5,9,10	21.5 (CH_3)	CH_3-20	1.23 (3H, *s*)	–	C-1, 5,9,10

The notations under Table 2 are as indicated in Table 1.

*2.3.6. ent-Labda-13(16),14-diene-3-one (**5**)*

Colourless oil; TLC, R_f: 0.31; GC, t_R = 13.36 min; elemental analysis, found: C, 83.31; H, 11.30; O, 5.58 ($C_{20}H_{32}O$ requires C, 83.27; H, 11.18; N, 5.55); UV (CH_3OH), λ_{max} (log ε) 320 (2.81) nm; IR cm^{-1}, ν_{max} (KBr): 3510, 3431 (OH), 2953, 2850 (methyl CH str.), 1750, 1705 (C=O cyclohexanone), 1450, 1352, 1263 cm^{-1} (C–O), 1718, (as. sec. C=O str.), 1750 (amide-I band, C=O str.), 1050, 920 (olefinic moiety); ^{1}H ($CDCl_3$, 300 MHz, δ ppm) and ^{13}C NMR ($CDCl_3$, δ ppm) (Table 3); EIMS, *m*/*z* (% rel. int.) 288 ([M]$^+$, 19), 269 (12), 235 (41), 122 (82), 97 (23), 166 (*100*), 98 (85).

*2.3.7. ent-Labda-13(16),14-diene (**6**)*

Yellowish oil; TLC, R_f: 0.56; GC, R_t: 6.57 min; elemental analysis, found: C, 87.67; H, 12.63 ($C_{20}H_{34}$ requires C, 87.52; H, 12.48); UV (CH_3OH), λ_{max} (log ε) 225 (3.11); IR cm^{-1}, ν_{max} (KBr): 3341, 2849, 2920 (methyl CH str.), 1720, 1710, 1452, 1369, 993, 885 (olefinic moiety), 739; ^{1}H ($CDCl_3$, 300 MHz, δ ppm) and ^{13}C NMR ($CDCl_3$, δ ppm) (Table 3); EIMS, *m*/*z* (% rel. int.) 274 ([M]$^+$, 16), 220 (38), 180 (*100*), 175 (58), 82 (69), 58 (10).

*2.3.8. ent-Labda-13(16),14-diene-3α-ol (**7**)*

Pale yellow oil; TLC, R_f: 0.40; GC, t_R = 10.25 min; elemental analysis, found: C, 82.89; H, 12.15; O, 5.52 ($C_{20}H_{34}O$ requires C, 82.70; H, 11.80; O, 5.51); UV (CH_3OH), λ_{max} (log ε) 227 nm (2.86); IR cm^{-1}, ν_{max} (KBr): 3550, 3446, 3459 (OH), 2915, 2850 (methyl CH str.), 1253 cm^{-1} (C–O), 1651, 1629, 1463, 1025 (olefinic moiety); ^{1}H ($CDCl_3$, 300 MHz, δ ppm) and ^{13}C NMR ($CDCl_3$, δ ppm) (Table 3); EIMS, *m*/*z* (rel. int.) 290 ([M]$^+$, 26); 229 (100), 191 (42), 150 (73), 137 (63), 121 (47).

2.4. In vitro antibacterial activity of the purified compounds and structure–activity correlation analyses

The bacterial strains used in this study were *V. parahaemolyticus* MTCC 451, *V. alginolyticus* MTCC 4439, and *V. vulnificus* MTCC 1145. The *in vitro* antibacterial activity of the compounds was tested by the disc-diffusion method (Bauer, Kirby, Scherris, & Turck, 1966), and minimum inhibitory concentration (MIC), as determined by microdilution method (Jones & Barry, 1987). For susceptibility testing, all the stock solutions were prepared in Me_2SO. For agar disc-diffusion assay, Zobell agar (10 ml) was introduced into sterile Petri dishes (90 mm diameter), and inoculated with 1 ml of 18 h 15‰ NaCl TSA broth culture (10^7 bact./ml). Blank paper discs (6 mm diameter, sterile blank) were impregnated with Me_2SO as blank, with test compounds (50, 100, and 150 μg loadings), which were placed on Petri plates containing Mueller Hinton agar impregnated with bacterial suspensions. The plates were incubated overnight at 37 °C and the antibacterial activity was defined as the diameter (in mm) of the clear inhibitory zone formed around the paper disc. Inhibition zones of >15 mm was declared as

Table 3
^{1}H NMR and ^{13}C NMR spectral data of compounds **5–7** (300 MHz, $CDCl_3$, DMSO-d_6, δ values)[a]; the δ values are in ppm.

C No.	Compound **5**				Compound **6**				Compound **7**			
	δ ^{13}C NMR[b]	H	δ ^{1}H NMR	HMBC	δ ^{13}C NMR[b]	H	δ ^{1}H NMR	HMBC	δ ^{13}C NMR[b]	H	δ ^{1}H NMR	HMBC
1	37.2 (CH_2)	1a	1.80 (1H, *m*)	C-3, 5	40.5 (CH_2)	1a	1.44 (1H, *m*)	–	34.9 (CH_2)	1a	1.59 (1H, *m*)	–
		1b	1.89 (1H, *t*, *J* = 5.4 Hz)	–		1b	1.50 (1H, *t*, *J* = 9.3 Hz)	–		1b	1.72 (1H, *m*)	–
2	34.8 (CH_2)	2a	2.24 (1H, *m*)	C-4, 6	19.1 (CH_2)	2a	1.35 (1H, *m*)	C-4, 10	28.4 (CH_2)	2a	1.75 (1H, *d*, *J* = 6.5 Hz)	C-10, 11
		2b	2.30 (1H, *t*, *J* = 2.6 Hz)	–		2b	1.39 (1H, *m*)	–		2b	1.68 (1H, *t*, *J* = 2.6 Hz)	–
3	220.1 (C)			C-4, 10	44.8 (CH_2)	3a	1.28 (1H, *t*, *J* = 12.1 Hz)	–	83.6 (CH)	3	3.20 (1H, *t*, *J* = 12.1 Hz)	–
				–		3b	1.32 (1H, *t*, *J* = 6.6 Hz)	–		3-OH	2.10 (1-OH, *bs*)	–
4	45.8 (C)			–	32.1 (C)			–	40.1 (C)			–
5	53.7 (CH)	5	1.65 (1H, *t*, *J* = 9.3 Hz)	C-4, 6	60.4 (CH)	5	1.45 (1H, *m*)	C-4, 10	55.3 (CH)	5	1.52 (1H, *t*, *J* = 9.3 Hz)	C-4, 10
6	15.3 (CH_2)	6a	1.85 (1H, *m*)	C-3, 5	19.9 (CH_2)	6a	1.30 (1H, *m*)	C-3, 5	22.8 (CH_2)	6a	1.25 (1H, *m*)	C-3, 5
		6b	1.92 (1H, *d*, *J* = 6.5 Hz)	–		6b	1.41 (1H, *d*, *J* = 2.6 Hz)	–		6b	1.38 (1H, *m*)	–
7	40.9 (CH_2)	7a	1.39 (1H, *m*)	–	34.7 (CH_2)	7a	1.30 (1H, *m*)	–	36.5 (CH_2)	7a	1.31 (1H, *m*)	–
		7b	1.46 (1H, *m*)	–		7b	1.41 (1H, *m*)	–		7b	1.46 (1H, *m*)	–
8	74.1 (CH)	8	1.73 (1H, *m*)	–	34.1 (CH)	8	1.68 (1H, *m*)	–	32.1 (CH)	8	1.62 (1H, *m*)	–
9	62.5 (CH)	9	1.60 (1H, *m*)	–	57.3 (CH)	9	1.50 (1H, *m*)	–	53.2 (CH)	9	1.42 (1H, *m*)	–
10	30.8 (C)			–	40.0 (C)			–	38.6 (C)			–
11	18.9 (CH_2)	11a	1.16 (1H, *t*, *J* = 2.1 Hz)	–	24.9 (CH_2)	11a	1.23 (1H, *t*, *J* = 2.6 Hz)	–	26.1 (CH_2)	11a	1.28 (1H, *t*, *J* = 3.1 Hz)	–
		11b	1.35 (1H, *m*)	–		11b	1.35 (1H, *m*)	–		11b	1.35 (1H, *m*)	–
12	32.6 (CH_2)	12a	2.08 (1H, *t*, *J* = 3.6 Hz)	C-10, 11	32.6 (CH_2)	12a	2.01 (1H, *t*, *J* = 3.6 Hz)	C-10, 14	35.2 (CH_2)	12a	1.92 (1H, *t*, *J* = 3.2 Hz)	C-10, 14
		12b	2.13 (1H, *t*, *J* = 2.8 Hz)	–		12b	2.06 (1H, *t*, *J* = 2.8 Hz)	–		12b	1.96 (1H, *t*, *J* = 2.6 Hz)	–
13	140.2 (C)			C-8, 9	145.2 (C)			C-6, 15	147.0 (C)			C-6, 15
				–				–				–
14	137.3 (CH)	14	6.11 (1H, *m*)	–	135.6 (CH)	14	6.28 (1H, *m*)	–	135.5 (CH)	14	6.30 (1H, *m*)	–
15	119.9 (CH_2)	15a	5.15 (1H, *t*, *J* = 6.6 Hz)	–	118.4 (CH_2)	15a	5.10 (1H, *t*, *J* = 5.4 Hz)	–	120.1 (CH_2)	15a	4.98 (1H, *t*, *J* = 6.2 Hz)	–
		15b	5.23 (1H, *m*)	–		15b	5.16 (1H, *m*)	–		15b	5.10 (1H, *m*)	–
16	112.0 (CH_2)	CH_2-16	4.85 (2H, *s*)	–	105.2 (CH_2)	CH_2-16	4.95 (2H, *s*)	–	106.3 (CH_2)	CH_2-16	4.85 (2H, *s*)	–
17	23.1 (CH_3)	CH_3-17	1.08 (3H, *s*)	–	20.5 (CH_3)	CH_3-17	1.03 (3H, *s*)	–	18.5 (CH_3)	CH_3-17	1.06 (3H, *s*)	–
18	24.7 (CH_3)	CH_3-18	1.25 (3H, *s*)	–	26.8 (CH_3)	CH_3-18	1.12 (3H, *s*)	–	20.3 (CH_3)	CH_3-18	1.09 (3H, *s*)	–
19	26.3 (CH_3)	CH_3-19	1.30 (3H, *s*)	–	28.0 (CH_3)	CH_3-19	1.24 (3H, *s*)	–	24.7 (CH_3)	CH_3-19	1.12 (3H, *s*)	–
20	19.2 (CH_3)	CH_3-20	1.12 (3H, *s*)	–	20.4 (CH_3)	CH_3-20	1.18 (3H, *s*)	–	23.7 (CH_3)	CH_3-20	1.20 (3H, *s*)	–

The notations under Table 3 are as indicated in Table 1.

strong, from 8 to 15 mm as moderate, and from 1 to 8 mm as weak activities. MIC values of test compounds and solvent fractions against the test bacterial strains were determined, using a microdilution method. The test compounds (0.5 mg) were diluted in Me_2SO (500 μl) and mixed with bacterial strains cultured in nutrient broths (9.5 ml). The initial concentration of test compounds was 4 mg/ml, and concentrations of 10, 20, 30, 40, 50, 60, 70, 80, 90, 100, 150, 200, and 250 μg/ml were obtained by serial dilutions. Antibacterial tests were performed by transferring each bioassay culture (10 ml bacterial culture with test compounds) into a new test tube containing only nutrient broth. Observations were made after 24 h to determine the possible bacterial growth in the respective culture broths. Optical density of treated cells reflects their viability and provides sufficient information pertaining to the mode of action of the tested metabolites.

Structure–activity correlation analyses were applied to two families of labdane diterpenoids containing an olefinic moiety in the side chain. Electronic and steric parameters were considered to explain structural moieties responsible for imparting bioactivity. Parachor was chosen as the bulk descriptor, whereas polarisability was taken as the electronic descriptor variable (Chakraborty & Devakumar, 2005).

2.5. Statistical analysis

Results of the bacterial counts were analysed using one-way analysis of variance (ANOVA), following the statistical programme for the social sciences (SPSS, ver. 13.0). A significance level of 95% ($p = 0.05$) was used throughout. All measurements were performed at least in triplicate ($n = 3$), and values were averaged.

3. Results and discussion

3.1. Chromatographic purification of secondary metabolites from *U. fasciata*

Amongst the three solvents used to extract the bioactive components of *U. fasciata*, dichloromathanic (CH_2Cl_2) extract exhibited maximum activity against the tested bacteria, followed

by ethylacetate (EtOAc, $CH_3COOC_2H_5$), and *n*-hexane extracts. The CH_2Cl_2 extract was concentrated under vacuum, which yielded a brown viscous oily residue. The residue (12.8 g) was fractionated by gradient neutral alumina open column chromatography, using 0–50% EtOAc/*n*-hexane. The chromatographic separation led to the isolation of four labdanes (**1–4**), and three *ent*-labdane diterpenoids (**5–7**), namely labda-14-ene-8-ol (**1**) (15.8 mg), labda-14-ene-3α,8α-diol (**2**) (10.8 mg), labda-14-ene-8α,9α-diol (**3**) (6.1 mg), labda-14-ene-8α-hydroxy-3-one (**4**) (8.2 mg), *ent*-labda-13(16),14-diene-3-one (**5**) (9.5 mg), *ent*-labda-13(16),14-diene (**6**) (12.0 mg), and *ent*-labda-13(16),14-diene-3α-ol (**7**) (11.6 mg) (Fig. 1).

3.2. Spectroscopic structural characterisation of chromatographically purified molecules from U. fasciata

3.2.1. General

The molecular structures of these secondary metabolites were proposed on the basis of comprehensive analysis of the 1D and 2D NMR (^{13}C, ^{1}H, ^{1}H–^{1}H COSY, HMQC, HMBC, and NOESY) and IR, UV, and mass spectra (Tables 1–3).

3.2.2. Labda-14-ene-8-ol (*1*)

This compound was obtained as a yellowish oil upon repeated column chromatography on alumina columns. The IR absorption band at 3415 cm^{-1} is due to the OH stretching vibrations. Its mass spectrum exhibited a molecular ion peak at *m*/*z* 292 which, in combination with its ^{1}H and ^{13}C NMR data, enabled us to assign the molecular formula of $C_{20}H_{36}O$, an oxygenated diterpenoid with three degrees of unsaturation. The ^{1}H NMR recorded five methyl singlets (δ 1.09 (*s*), 1.37 (*s*), 0.93 (*s*), 0.98 (*s*), and 1.19 (*s*) due to CH_3-16, CH_3-17, CH_3-18, CH_3-19, and CH_3-20, respectively), and methine multiplets at δ 1.67 (1H, *m*, H-5), δ 1.52 (1H, *dd*, H-9), and δ 2.31 (1H, *m*, H-13) (Table 1). The resonances of several methylene protons connected to the same carbon at different chemical shifts substantiate the presence of fused bicyclic rings in the molecule, as is evident from the ^{1}H NMR spectrum (Table 1). The ^{1}H NMR signals of **1** indicate that one of the unsaturations was due to the side chain olefinic moiety, and the other two due to the two rings, since no signal arising from multiple bonds was present in the spectra. The presence of a methine carbinol group (H-8) was also observed at δ 2.20 (1H, *bs*). The remaining proton signals were overlapping in the range of δ 1.20–1.70. These include six

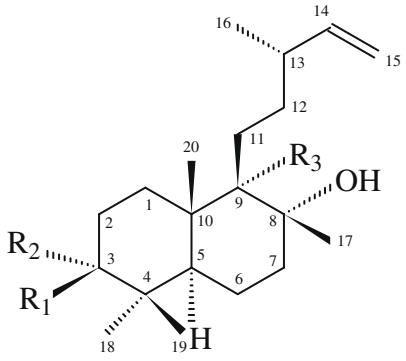

Compounds 1-4

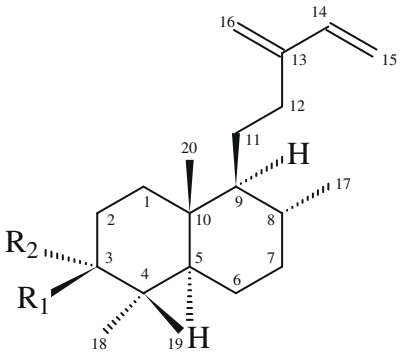

Compounds 5-7

Compound Number	R_1	R_2	R_3
1	H	H	H
2	OH	H	H
3	H	H	OH
4	=O	-	H
5	=O	-	-
6	H	H	-
7	H	OH	-

Fig. 1. Structural variations of labdane diterpenoids isolated from *Ulva fasciata*.

methylene and two methine protons. The ^{13}C NMR spectrum, supported by DEPT experiments, also showed well-resolved resonances for all the 20 carbon atoms, suggesting the structure of a diterpene (Table 1). The ^{13}C NMR spectrum also displayed signals characteristic of one double bond at C-14 (δ 136.4, *d* and 114.8, *s*) (Table 1). Two of the primary methyl groups, (H_3-18) and (H_3-19), were found to be *geminal*, as indicated by couplings between the two groups in the HMBC spectrum, suggesting that the tertiary hydroxyl group is at C-8 on the B-ring of the molecule. This conclusion is in accordance with the HMBC correlations of the congeneric diterpenoid skeleton (Nagashima & Asakawa, 2001). The relative stereochemistry of the chiral centres at C-5, C-8, C-9, and C-10 was deduced from the NOESY spectrum of the compound and the *J* values, and the results were validated with related compounds in the literature (Khalil, Gedara, Lahloub, & Halim, 1996). Couplings were apparent between H-3/H_3-18 and H-3/H_a-5, indicating that H-3 must be equatorial and on the α-side of the molecule. This was also supported by the large *J* values for the equatorial–axial and equatorial–equatorial couplings between H-3/H_a-2 and H-3/H_b-2 (Nagashima & Asakawa, 2001). The presence of NOESY couplings (H-5/H_3-19) indicates that H-5 had to be α-oriented like the C-18 methyl. NOESY correlations between H-17/H_3-20 and H-9/H_3-16 indicate the close proximity of these groups, and their α-disposition. Therefore, the C-17 methyl group had to be axial and β-oriented. The proton-bearing carbon signals were assigned by analysis of the HMQC spectrum and the correlations observed in the HMBC spectrum confirm the planar structure of **1**. Based upon these interpretations and literature data (Nagashima & Asakawa, 2001; Ngadjui et al., 1999), the compound **1** was identified as labda-14-ene-8-ol.

3.2.3. Labda-14-ene-3α,8α-diol (*2*)

Compound **2** belonged to a series of similar labdanes (**1–4**). The IR spectrum showed absorption bands (3450 cm^{-1} *br*) recording the presence of hydroxyl groups. The band at 1530 cm^{-1} is the resultant of the interactions between OH bending and CH stretching vibrations. The EIMS spectrum, associated with NMR spectra and comparison of literature data, suggests that compound **2** is an oxygenated diterpene (Roengsumran et al., 2001). The mass spectrum exhibited a molecular ion peak at *m/z* 308 with three degrees of unsaturation. The fragment ion at *m/z* 140 (2,2,4-trimethyl cyclohex-3-enol) is due to the elimination of $C_3H_6O]^+$ and $C_6H_{10}]^+$ from the $[M]^+$ ion. This ion may be formed by cleavage of the C9–C11 bond, transfer of hydrogen, and breaking of the C5–C6 and C-7 and C-8 bonds with the elimination of a water molecule (−18 amu) in a rearrangement reaction. The base peak at *m/z* 166 (100%) may be formed by the elimination of the side chain at C9, as well as elimination of the OH and methyl groups from decahydro-1,1,4,6-tetramethyl-5-vinylnaphthalene (*m/z* = 220). The ^1H and ^{13}C NMR spectra of **1** and **2** are very similar, suggesting that both compounds have closely related molecular structures. The ^{13}C NMR spectrum of **2**, along with DEPT experiments, revealed the presence of five methyl groups, seven methylene groups, five methine groups, and three quarternary carbons, indicating the presence of 33 hydrogen atoms connected to carbon atoms (Table 1). The ^{13}C NMR spectrum also displayed signals characteristic of one double bond at δ 139.2 (*d*) and 118.6 (*s*) (Table 1). The signal at δ 71.5 was assigned to a quarternary carbon bonded to an OH group at C-8. All the spectral data, in combination with the NMR spectral data of related diterpenoids (Nagashima & Asakawa, 2001; Li et al., 2002), enabled us to elucidate the compound as bicyclic. The ^1H NMR and ^{13}C NMR spectral chemical shifts were assigned through direct and long-range C–H correlations, using HMBC, HMQC techniques and COSY. Analysis of 2D NMR (^1H–^1H COSY, HSQC and HMBC) spectra revealed diagnostic ^1H–^1H COSY correlations between the carbinolic proton at H-3 (δ 3.27, *t*, *J* = 6.4 Hz) and olefinic proton H-2 (δ 1.76 in H1; δ 1.89 in H2). Diagnostic ^1H–^1H COSY correlations were also apparent between H_2-6 (δ 1.40 in H1 and δ 1.59 in H2) and H_2-7 (δ 1.50 in H1 and δ 1.56 in H2). Other correlations between H-9 (δ 1.65, *m*), H_2-11 and H_2-12 are also apparent. By examination of the HMBC and ^1H–^1H COSY spectra, the position of the secondary alcohol was assigned to C-3. The proton that was attached to the secondary hydroxy function appeared at δ 3.27 as a broad singlet. Hydrogen bonding apparently decreases the electron density around the proton, and thus moves the proton absorption to a lower field. The –CH_3 group at C-18 exhibited a downfield shift (δ 1.06, *s*, 3H) because of the vicinal –OH group. The A–B *cis*-fused structures were proposed on the basis of low field ^{13}C NMR signals of the bridgehead methyl carbons (δ 23.4), and the results were validated with related diterpenoid skeletons in the existing literature (Roengsumran et al., 2001; Nagashima & Asakawa, 2001; Li et al., 2002). The relative stereochemistry of all the stereogenic centres was derived from the NOESY spectrum. In the NOESY spectrum, significant NOE effects were apparent between Me-20 and H-11, Me-20 and H_3-16, Me-8 and H-12, Me-20 and H_3-19, Me-18 and H-5. The carbon chemical shift of CH_3-17 enabled us to assign its stereochemistry as equatorial. These interpretations, in combination with the literature data of related diterpenoid skeleton (Roengsumran et al., 2001), led to the assignment of the structure of labda-14-ene-3α,8α-diol (**2**).

3.2.4. Labda-14-ene-8α,9α-diol (*3*)

Compound **3** was deduced to be an isomer of compound **2**. The IR absorption band at 3550 cm^{-1} is due to the OH stretching vibrations. The signal at 2896 cm^{-1} is due to the methyl CH stretching vibrations. The typical ^1H NMR shifts of protons of **3** are recorded in Table 2. In the ^1H NMR spectrum, the most downfield methyl signal (CH_3-17) appeared at δ 1.68, and was bound to the oxygen-bearing carbon (δ 86.9) C8, apparently due to hydrogen bonding that decreases the electron density around the proton, and thus moves the proton absorption to a lower field (Table 2). The ^{13}C NMR, along with DEPT experiments, exhibited 20 carbon signals derived from three quarternary carbons, four methines, eight methylenes, and five methyls (Table 2). The rest of the molecule and ^1H–^{13}C connectivities were further established by HMQC and HMBC experiments. HMBC data were used to confirm the moieties A and B, and established the connectivity between the protons and carbon atoms (Li et al., 2002). The correlation of signals at δ 1.68 (H_3-17)/1.21 (H_3-20) with 25.3 (C-11), as well as the correlated signals at δ 1.08 (H-18)/1.13 (H-19)/1.21 (H_3-20) with δ 58.4 (C-5) were apparent in the HMBC spectrum of **3**. HMBC correlations were also apparent between δ 26.3 (C-18) with δ 1.54 (H-5), δ 27.4 (C-19) with δ 1.21 (H_3-20). The relative stereochemistry was assigned on the basis of a study of the coupling constants and NOESY experiments. A strong correlation between H-5 and H_3-4, as evident from the NOESY spectrum, was observed that confirmed their equatorial disposition. NOE interactions were also apparent between H_3-20/H-11/H_3-17, which are in agreement with these methyl and methylene groups being in the axial position (Khalil et al., 1996). The β-configuration at C-9 was deduced from the NOESY correlations between Me-20 and H-11a and H-11b of the side chain. Based upon these interpretations and supporting literature data (Khalil et al., 1996; Li et al., 2002), the compound **3** was identified as labda-14-ene-8α,9α-diol (**3**).

3.2.5. Labda-14-ene-8α-hydroxy-3-one (*4*)

The IR spectrum of compound **4**, a colourless oil revealed a prominent absorption band at ν_{max} 1705 cm^{-1}, attributed to carbonyl functionality. The molecular formula, $C_{20}H_{34}O_2$, of **4** was determined by the analysis of the EIMS spectrum (*m/z* 306) and ^{13}C NMR spectral data, including 2D NMR. The presence of a car-

bonyl group was apparent by IR spectrometry (1710 cm^{-1}) and the ^{13}C NMR spectrum, which showed a signal at δ 221.4 (Table 2). The ^{1}H and ^{13}C NMR spectra showed, besides resonances for the olefinic side chain, the signals of one tertiary hydroxyl group (δ 76.8) and five singlet methyls (δ 24.5, 26.9, 23.3, 25.6, and 21.5). Correlations of H-2α, H-2β, H-3β, and CH_3-20 with the carbonyl function in the HMBC spectrum led to the assignment of the ketone to C-3. CH_3-17 was deshielded (δ 1.35) because of its close vicinity to the ketone, and was shifted downfield. Since the HMBC spectrum exhibited correlations between H-6β, H-7β, H-11α, and H-11β and the carbon at δ 76.8, it was assigned to be C-8, and was deduced to carry the methyl at δ 1.35. The correlation of CH_3-20 with H-11α as in the NOESY spectrum provided evidence for the β-configuration of C-9. The proton-bearing carbon signals were assigned by the HMQC spectrum, and compared with the related literature data (Sob, Tane, Ngadjui, Connolly, & Ma, 2007; Tanaka et al., 2000) to assign the compound as labda-14-ene-8α-hydroxy-3-one (**4**).

3.2.6. ent-Labda-13(16),14-diene-3-one (**5**)

The IR spectrum of compound **5**, a colourless oil, revealed prominent absorption bands at ν_{max} 3510 and 1705 cm^{-1}, attributed to hydroxyl and carbonyl groups, respectively. In addition, a strong IR absorption at 3431 cm^{-1}, indicative of hydroxyl groups, and intense bands at 1750 cm^{-1}, indicated carbonyl function. The ^{1}H NMR spectrum showed exchangeable protons, methyl groups (two secondary and three quarternary), and complex proton resonances between δ 1.39 and 2.30, suggestive of a bicyclic diterpenoid structure (Table 3) (Nagashima, Takaoka, & Asakawa, 1998). The presence of bicyclohexanone protons was validated by typical methylene signals in the ^{1}H NMR spectrum [δ_H 1.80 (1H, *m*), 1.89 (1H, *t*, *J* = 5.4 Hz), 2.24 (1H, *m*), 2.30 (1H, *t*, *J* = 2.60 Hz), 1.85 (1H, *m*), 1.92 (1H, *d*, *J* = 6.5 Hz), 1.39 (1H, *m*), and 1.46 (1H, *m*)] (Table 3). The ^{13}C NMR spectrum exhibited signals for all the 20 carbons, including the following: one quarternary vinyl carbon (δ_C 140.2), one oxygenated quarternary carbon (δ_C 220.1), eight methylenes (δ_C 37.2, 34.8, 15.3, 40.9, 18.9, 32.6, 119.9, and 112.0), four methine carbons (δ_C 53.7, 74.1, 62.5, 137.3), and four methyl groups (δ_C 23.1, 24.7, 26.3, 19.2) (Table 3). The sequences of hydrogen and carbon atoms of rings A and B were established by ^{1}H–^{1}H COSY and HMBC. HMBC long-range correlations of H_3-20 (δ 1.12) and H-11 (δ 1.35) with C-10 (δ_C 30.8), and those of H-9 (δ 1.60) with both C-12 (δ_C 32.6) and C-11 (δ 18.9), enabled the olefinic side chain to be linked to C-9. In the same way, the relative stereochemistry of the ring substituents in C-1, C-3, C-6, C-7, C-9, C-10, and C-15 was determined by a combination of NMR methods. Detailed analysis of the NMR spectra, along with comparison of literature data (Carreras, Rossomando, & Giordano, 1998), indicated that the compound has a 13(16) double bond. The long-ranged COSY correlations, H-8/H-7, CH_3-17/αH-15, αH5/αH7, and H5/H-8, suggest the equatorial position of CH_3-17, and the chair conformation of the fused bicyclic rings A and B (Khalil et al., 1996). Moreover, the axial position of CH_3-20 was proved by the ^{1}H–^{1}H COSY long-range correlation between H_3-20/H-1β. Based upon the structural interpretations and existing literature data (Carreras et al., 1998), **5** has been elucidated to be as *ent*-labda-13(16),14-diene-2-one.

3.2.7. ent-Labda-13(16),14-diene (**6**)

The ^{1}H and ^{13}C NMR spectra of **6** (*m*/*z* 274 $[M]^+$, $C_{20}H_{34}$) exhibited signals for an olefinic methylene group (δ 5.10, *t*, *J* = 5.4 Hz; δ 5.16, *m*), a vinyl group (δ 6.28, *m*; δ 5.10, *t*, *J* = 5.4 Hz; δ 5.16, *m*), and four singlet methyls (CH_3-17, CH_3-18, CH_3-19, and CH_3-20 at δ 1.03, 1.12, 1.24, and 1.18) (Table 3). All the proton and carbon signals were assigned using a combination of ^{1}H–^{1}H COSY, HSQC, and HMBC experiments. The ^{13}C NMR data of **5** and **6** were consistent with the reported ^{13}C shift differences between axial and equatorial methyl groups of methylcyclohexane (Nagashima et al., 1998). HMBC long-range correlations of H-12 (δ_H 2.06) and H-11 (δ_H 1.23) with C-10 (δ_C 40.0) and those of H-9 (δ_H 1.50) with both C-11 (δ 24.9) and C-12 (δ_C 32.6) led us to conclude that the side chain is linked to C-9. This conclusion is in accordance with the related literature data (Nagashima et al., 1998; Carreras et al., 1998). The relative stereochemistry of the ring substituents in C-1, C-3, C-6, C-7, C-9, C-10, and C-15 was determined to be the same as that found in **5**. The ^{13}C shift of the axial methyl group at C-17 is 6 ppm to higher field than that of the deshielded equatorial methyl group at C-18, which apparently indicates the close vicinity of the former (CH_3-17) to an electronegative –OH group. These interpretations are in agreement with the similar hydroxylated diterpenoid skeletons reported earlier (Nagashima & Asakawa, 2001; Carreras et al., 1998). Based upon these interpretations and related literature data, the compound **6** is elucidated as *ent*-labda-13(16),14-diene.

3.2.8. ent-Labda-13(16),14-diene-3α-ol (**7**)

The IR spectrum of **7** showed characteristic hydroxyl bands at 2550 and 3446 cm^{-1}. A weak band at 1253 cm^{-1} also apparently results from the OH bending and CH stretching interactions. The EIMS spectrum exhibited a peak at *m*/*z* 290, consistent with the molecular formula of $C_{20}H_{34}O$, and hence four double bond equivalents, as represented by two olefinic double bonds (δ 147.0, δ 135.5, δ 6.30, *m*; and δ 120.1, δ 4.98, *t*; δ 5.10, *m*; and δ 106.3, δ 4.85, *s*), and two rings. These interpretations are based on NMR experiments and related literature data (Sob et al., 2007; Tanaka et al., 2000). The singlet methyl at C-10 (δ 1.20) in the ^{1}H NMR spectrum was assigned as positioned at the ring junction (Table 3). Due to its downfield shift, the methyl at δ 1.09 was assigned to be *geminal* to the hydroxyl group. The ^{13}C NMR spectrum revealed a primary alcohol at C-3 (δ 83.6) in accordance with the resonances of a hydroxylic methine (δ 3.20, *J* = 12.1 Hz) in the ^{1}H NMR spectrum. The HMBC spectrum revealed the methyl at C-18 (δ 1.09) to be *geminal* to the hydroxymethylene group at C-3 (δ 83.6). Compound **7** has an equatorial tertiary hydroxyl group at C-3 and an axial CH_3-17 (δ 1.06, *s*). All these features were represented by the diterpenoid skeletons of *ent*-labdane type, and compared with literature data of related diterpenoid skeletons (Nagashima & Asakawa, 2001; Ngadjui et al., 1999; Carreras et al., 1998) to assign compound **7** as *ent*-labda-13(16),14-diene-3α-ol.

3.3. Effect of labdane derivatives on in vitro antibacterial activity and structure–activity relationship analyses

3.3.1. General

Structure–activity relationship (SAR) analysis is a useful tool in elucidating essential structural features governing macromolecular receptor in the target organism (bacteria) controlling antibacterial activity of the compounds (Chakraborty & Devakumar, 2006). The current SAR modelling approach focuses on whether the pharmacophores represented by the purified diterpenoids are active via related mechanisms. *V. parahaemolyticus* MTCC 451 and *V. alginolyticus* MTCC 4439 were found to be more sensitive to all the compounds than was *V. vulnificus* MTCC 1145 (Table 4).

3.3.2. Antibacterial activity of the labdane diterpenoids (**1–4**) and structure–activity relationship study

Amongst labdane series, labda-14-ene-3α,8α-diol (**2**) exhibited significant activity ($p = 0.05$) against *V. parahaemolyticus* MTCC 451 and *V. alginolyticus* MTCC 4439 (zone sizes: 12 mm and 10 mm, respectively with 100 μg loading; MIC: 30 μg/ml). It can be inferred that highly electronegative groups, namely unhindered OH at C-3 and C-8 positions of the fused bicyclic ring system, undergo

Table 4
In vitro antibacterial activity of isolated compounds (**1–7**) as purified by column chromatography on neutral alumina on three fish pathogenic *Vibrio* sp.

C. No.[a]	*Vibrio parahaemolyticus* MTCC 451				*Vibrio vulnificus* MTCC 1145				*Vibrio alginolyticus* MTCC 4439			
	IZD (mm)[b]			MIC (μg/ml)	IZD (mm)[b]			MIC (μg/ml)	IZD (mm)[b]			MIC (μg/ml)
	50 μg	100 μg	150 μg		50 μg	100 μg	150 μg		50 μg	100 μg	150 μg	
1	NA	NA	NA	200	NA	NA	NA	200	NA	NA	NA	200
2	10.00 ± 0.20	12.00 ± 0.95	13.00 ± 0.17	30	8.30 ± 0.44	9.37 ± 0.57	9.73 ± 0.83	50	9.37 ± 0.45	11.7 ± 1.54	11.8 ± 1.89	30
3	7.43 ± 0.59	8.83 ± 0.38	9.37 ± 0.71	80	NA	NA	7.80 ± 0.92	150	7.03 ± 0.97	8.70 ± 0.44	9.38 ± 0.72	90
4	7.43 ± 0.61	9.93 ± 0.12	10.37 ± 0.74	50	6.37 ± 0.64	7.30 ± 0.44	8.60 ± 0.62	70	7.73 ± 0.72	9.37 ± 0.40	9.67 ± 1.27	80
5	6.23 ± 0.25	7.30 ± 0.70	7.30 ± 0.70	150	NA	NA	7.00 ± 0.00	150	6.37 ± 0.64	6.63 ± 0.57	7.00 ± 0.00	150
6	NA	NA	NA	250	NA	NA	NA	250	NA	NA	NA	250
7	7.47 ± 0.55	8.70 ± 0.62	8.93 ± 0.12	60	6.63 ± 0.57	7.40 ± 0.66	8.37 ± 0.90	80	8.03 ± 1.17	8.63 ± 0.61	9.63 ± 0.58	80

[a]C. No. indicates compound number; [b]IZD implies inhibition zone diameter expressed as mm, inhibition zone diameters are indicated at three different loadings (50, 100, and 150 μg) of test compounds; results are expressed as inhibition of bacterial growth (inhibition zone diameter in mm) and MIC (μg/ml) as determined by broth microdilution assay at different concentrations of test compounds (10–250 μg/ml). NA signifies no activity.

proton exchange reaction with the basic $-NH_2$ group (as in the histidyl residue) in the enzyme active site, resulting in protonation of the active amino group(s) (Fig. 2). The increased electrophilicity at the enzyme active site of pathogenic bacteria possibly results in lowering of virulence of the enzyme activity. Surprisingly, labda-14-ene-8α,9α-diol (**3**) has relatively lower activity (zone sizes: 9 mm and 8 mm, respectively against *V. parahaemolyticus* MTCC 451 and *V. alginolyticus* MTCC 4439, respectively with 100 μg loading; MIC: 80 and 90 μg/ml against the two bacteria) as compared to that of labda-14-ene-3α,8α-diol (**2**). This may be ascribed to the fact that the hydroxyl group at C-9 is sterically hindered by adjacent methyl (at C-9) and hydroxyl (C_3–OH) groups, resulting in an unfavourable conformational change in the macromolecular receptor site. It is apparent that, though polarisabilities of **2** and **3** are comparable ($\sim 37.00 \times 10^{-24}$ cm^3), the parachor (bulk descriptor) of the former (781.4 cm^3) is comparatively less than that of the latter ($P = 785.7$ cm^3). The increased bulk is due to the presence of –OH groups at C-8 and C-9, resulting in a less efficient macromolecular receptor-fit at the enzyme active site, and resulting in lower activity of compound **3** than compound **2**. The bulk parameter recorded a value of as high as 595.4 cm^3 for the decahydro-1,2,5,8a-pentamethyl naphthalene-1,2-diol moiety in labda-14-ene-8α,9α-diol (**3**) as compared to $P = 591.0$ cm^3 in the decahydro-1,1,4a,5,6-pentamethyl naphthalene-2,6-diol fragment in labda-14-ene-3α,8α-diol (**2**). The activities of labda-14-ene-8α-hydroxy-3-one (**4**) against *V. parahaemolyticus* MTCC 451 (zone size: 10 mm with 100 μg loading; MIC: 50 μg/ml) and *V. alginolyticus* MTCC 4439 (zone size: 9 mm with 100 μg loading; MIC: 80 μg/ml) are comparable to that of labda-14-ene-3α,8α-diol (**2**), apparently due to their structural similarity. It is hypothesised that the carbonyl functionality at C-3 of the octahydro-6-hydroxy-1,1,4a,5,6-pentamethyl naphthalene-2-(1H)-one moiety of labda-14-ene-8α-hydroxy-3-one (**4**) undergoes a reversible keto-enol tautomerism, resulting in the formation of a compound closely similar to that of labda-14-ene-3α,8α-diol (**2**), However, the activity of compound **4** was found to be comparatively less than that of compound **2**, presumably due to low polarisability ($\sim 36.4 \times 10^{-24}$ cm^3) caused by the absence of an active –OH group. Though labda-14-ene-8-ol (**1**) in this series exhibited optimum bioreceptor-fit, the lower activity against *V. parahaemolyticus* MTCC 451 (zone size: 6 mm with 100 μg loading; MIC: 200 μg/ml) and *V. alginolyticus* MTCC 4439 (zone size: 6 mm with 100 μg loading; MIC: >200 μg/ml) is attributed to the absence of an active (electronegative –OH group) functionality at unhindered C-3 position.

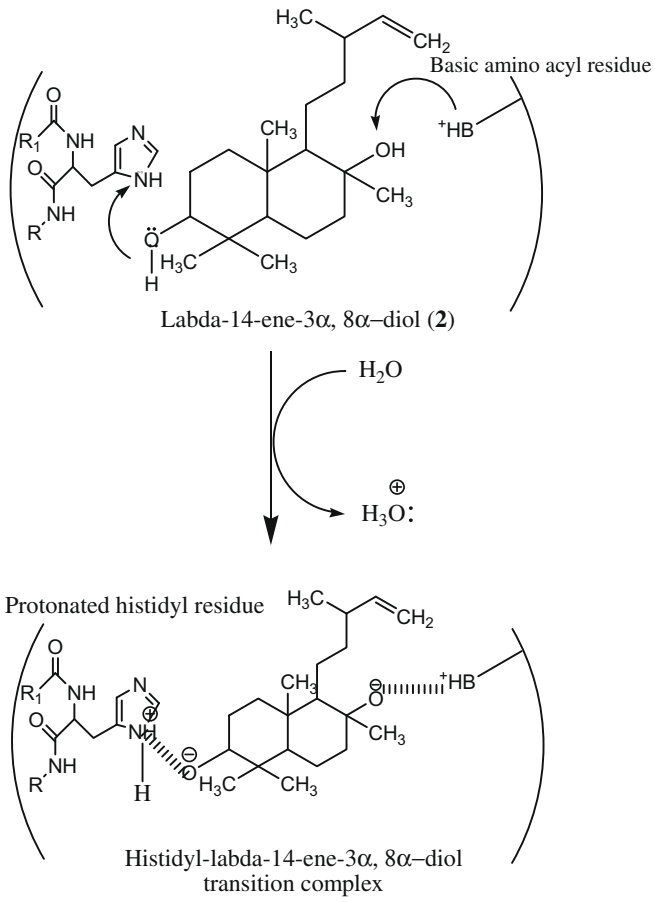

Fig. 2. Probable inhibition mechanism of labda-14-ene-3α,8α-diol (**2**) by protonation of basic aminoacyl (e.g., histidyl) residues inside enzyme active site on virulent enzymes of pathogenic bacteria. The highly electronegative group of **2** shed the electron cloud from basic aminoacyl residues in the enzyme active site, thus acting as a nucleophilic centre of the molecule, indicating a high level of activity.

3.3.3. Antibacterial activity of the ent-labdanes (**5–7**) and structure–activity relationship study

The *ent*-labdane series exhibited comparatively lower activity than the labdane series. Though *ent*-labda-13(16),14-diene-3-one (**5**), in this series, is structurally similar to labda-14-ene-8α-hydroxy-3-one (**4**) except for one extra olefinic group at the C14(16) position in the 3-methylene-hex-1-ene side chain, the former was found to exhibit lower activity against *V. parahaemolyticus* MTCC 451 (zone size: 7 mm with 100 μg loading; MIC: 150 μg/ml) and *V. alginolyticus* MTCC 4439 (zone size: 6 mm with 100 μg loading; MIC: 150 μg/ml) than the latter. This result may be attributed to the fact that the olefinic double bond at C14(16), being in the "Z"

configuration, has a less efficient macromolecular receptor-fit than that of compound **4**, which has only one olefinic group at C-14. This hypothesis is further substantiated by the fact that the 3-methylene-hex-1-ene moiety, as in compound **5**, has a lower polarisability ($\sim 13.38 \times 10^{-24}$ cm^3) than that of 3-methyl hex-1-ene moiety in compound **4** ($\sim 13.54 \times 10^{-24}$ cm^3). Amongst *ent*-labdane derivatives, *ent*-labda-13(16),14-diene-3α-ol (**7**) exhibited the highest activity (zone sizes: 9 mm against *V. parahaemolyticus* MTCC 451 and *V. alginolyticus* MTCC 4439, with 100 μg loading; MIC: 60 and 80 μg/ml, respectively against the two bacteria), due to an active hydroxyl group at the C-3 position of the fused bicyclic ring. It is likely that the highly electronegative group ($O_{E.N.} = 3.50$) shed the electron cloud from basic amino acyl residues in the enzyme active site and thus acted as a nucleophilic centre of the molecule, indicating a high level of activity. *ent*-Labda-13(16),14-diene (**6**) has recorded the lowest activity in this series (MIC: ~250 μg/ml against all the test bacteria) (Table 4), obviously due to the absence of any electronegative groups in the fused bicyclic ring system (decahydro-1,1,4a,5,6-pentamethyl naphthalene moiety).

4. Conclusions

Seven labdane diterpenoids, namely labda-14-ene-8-ol (**1**), labda-14-ene-3α,8α-diol (**2**), labda-14-ene-8α,9α-diol (**3**) labda-14-ene-8α-hydroxy-3-one (**4**), *ent*-labda-13(16),14-diene-2-one (**5**), *ent*-labda-13(16),14-diene-3α-ol (**6**), and *ent*-labda-13(16),14-diene-3α-ol (**7**), were isolated as major constituents, by chromatography of the CH_2Cl_2/CH_3OH (1:1, v/v)-soluble fraction of *U. fasciata* (Chlorophyceae) Delile on neutral alumina, using various mixtures of EtOAc and *n*-hexane (0–50% EtOAc/*n*-hexane) as eluents. Structures of these secondary metabolites were established using spectroscopic analysis, especially IR, mass, and NMR spectra, in conjunction with 2D NMR experiments, namely ^1H–^1H COSY, HMQC, and heteronuclear correlation techniques. The relative stereochemistry was assigned on the basis of a study of the coupling constants and NOESY experiments. The *in vitro* antibacterial activity of these secondary metabolites was evaluated against three fish pathogenic bacteria, namely *V. parahaemolyticus* MTCC 451, *V. alginolyticus* MTCC 4439, and *V. vulnificus* MTCC 1145. The antibacterial assay revealed that labdane derivatives (**1–4**) were superior to *ent*-labdane derivatives (**5–7**). Two labdane diterpenoids, namely labda-14-ene-3α,8α-diol (**2**) and labda-14-ene-8α-hydroxy-3-one (4) were found to be potent antibacterial constituents of this alga, and exhibited higher activity against *V. parahaemolyticus* and *V. harveyii* (MIC: 30 μg/ml) than did other compounds. Structure–activity relationships revealed that the compounds with electronegative hydroxyl or carbonyl group(s) exhibit greater activities, apparently by proton exchange reactions with the basic amino acyl residue at the enzyme active site of virulent enzymes of pathogenic bacteria. This study may lead to promising antibacterial molecules against infections with multi-resistant Gram-negative fish pathogenic bacteria, and explain the primary site and mode of action of this class of diterpenoids.

Acknowledgements

The authors are thankful to Prof. Dr. Mohan Joseph Modayil, Director, CMFRI, Cochin for providing necessary facilities to carry out the work. Thanks are also due to Dr. Shibu M. Eappen, Scientist B, Sophisticated Test and Instrumentation Centre, Cochin University of Science and Technology, Kerala for recording the mass spectral data. The authors thank Dr. S. Saravanan, Doctoral fellow of Madurai Kamaraj University for recording NMR spectra.

References

Anjaneyulu, A. S. R., Prakash, C. V. S., & Mallavadhani, U. V. (1991). Two caulerpin analogues and a sesquiterpene from *Caulerpa racemosa*. *Phytochemistry, 30*, 3041–3042.

Awad, N. E. (2000). Biologically active steroid from the green alga *Ulva lactuca*. *Phytotherapy Research, 14*, 641–643.

Bauer, A. W., Kirby, W. M. M., Scherris, J. C., & Turck, M. (1966). Antibiotic susceptibility testing by a standardized single disc method. *American Journal of Clinical Pathology, 45*, 493–496.

Blunt, J. W., Copp, B. R., Munro, M. H. G., Northcote, P. T., & Prinsep, M. R. (2006). Marine natural products. *Natural Product Reports, 23*, 26–78.

Carreras, C. R., Rossomando, P. C., & Giordano, O. S. (1998). *Ent*-labdanes from *Eupatorium buniifolium*. *Phytochemistry, 48*, 1031–1034.

Chakraborty, K., & Devakumar, C. (2005). Quantitative structure–activity relationship analysis as a tool to evaluate the mode of action of chemical hybridizing agents for wheat (*Triticum aestivum* L.). *Journal of Agricultural and Food Chemistry, 53*, 3468–3475.

Chakraborty, K., & Devakumar, C. (2006). Chemical hybridizing agents for chickpea (*Cicer arietinum* L.): Leads from QSAR analysis of ethyl oxanilates and pyridones. *Journal of Agricultural and Food Chemistry, 54*, 1868–1873.

Farooqi, A. H. A., Shukla, Y. N., Shukla, A., & Bhakuni, D. S. (1990). Cytokinins from marine organisms. *Phytochemistry, 29*, 2061–2063.

Flodin, C., & Whitfield, F. B. (1999). 4-Hydroxybenzoic acid: A likely precursor of 2,4,6-tribromophenol in *Ulva lactuca*. *Phytochemistry, 51*, 249–255.

Guerriero, A., Marchetti, F., Ambrosio, M. D., Senesi, S., Dini, F., & Pietra, F. (1993). New ecotoxicologically and biogenetically relevant terpenes of the tropical green seaweed *Caulerpa taxifolia* which is invading the Mediterranean. *Helvetica Chimica Acta, 76*, 855–864.

Hamann, M. T., & Scheuer, P. J. (1993). Kahalalide F: A bioactive depsipeptide from the sacoglossan mollusk *Elysia rufescens* and the alga *Bryopsis* sp. *Journal of American Chemical Society, 115*, 5825–5826.

Handley, J. T., & Blackman, A. J. (2000). Monocyclic diterpenes from the marine alga *Caulerpa trifaria* (Chlorophyta). *Australian Journal of Chemistry, 53*, 67–71.

Handley, J. T., & Blackman, A. J. (2005). Secondary metabolites from the marine alga *Caulerpa brownii* (Chlorophyta). *Australian Journal of Chemistry, 58*, 39–46.

Jones, R. N., & Barry, A. L. (1987). The antimicrobial activity of A-56268 (TE-031) and roxithromycin (RU965) against *Legionella* using broth micro dilution method. *Journal of Antimicrobial Chemotherapy, 19*, 841–842.

Khalil, A. T., Gedara, S. R., Lahloub, M. F., & Halim, A. F. (1996). Diterpenes and a flavone from *Leucas neufliseana*. *Phytochemistry, 41*, 1569–1571.

Koehn, F. E., Gunasekera, S. P., Neil, D. N., & Cross, S. S. (1991). Halitunal, an unusual diterpene aldehyder from the marine alga *Halimeda tuna*. *Tetrahedron Letters, 32*, 169–172.

Li, S. H., Zhang, H. J., Qiu, S. X., Niu, X. M., Santarsiero, B. D., Mesecar, A. D., et al. (2002). Vitexlactam A, a novel labdane diterpene lactam from the fruits of *Vitex agnuscastus*. *Tetrahedron Letters, 43*, 5131–5134.

Nagashima, F., & Asakawa, Y. (2001). Sesqui- and diterpenoids from two Japanese and three European liverworts. *Phytochemistry, 56*, 347–352.

Nagashima, F., Takaoka, S., & Asakawa, Y. (1998). Diterpenoids from the Japanese liverwort *Jungermannia infusca*. *Phytochemistry, 49*, 601–608.

Ngadjui, B. T., Folefoc, G. G., Keumedjio, F., Dongo, E., Sondengam, B. L., & Connolly, J. D. (1999). Crotonadiol, a labdane diterpenoid from the stem bark of *Croton zambesicus*. *Phytochemistry, 51*, 171–174.

Paul, V. J., Cronan, J. M., Jr., & Cardellina, J. H. II, (1993). Isolation of new brominated sesquiterpene feeding deterrents from tropical green alga *Neomeris annulata* (Dasycladaceae: Chlorophyta). *Journal of Chemical Ecology, 19*, 1847–1860.

Puglisi, M. P., Tan, L. T., Jensen, P. R., & Fenical, W. (2004). Capisterones A and B from the tropical green alga *Penicillus capitatus*: Unexpected anti-fungal defenses targeting the marine pathogen *Lindra thallasiae*. *Tetrahedron, 60*, 7035–7039.

Roengsumran, S., Petsom, A., Kuptiyanuwat, N., Vilaivan, T., Ngamrojnavanich, N., Chaichantipyuth, C., et al. (2001). Cytotoxic labdane diterpenoids from *Croton oblongifolius*. *Phytochemistry, 56*, 103–107.

Selvin, R., Huxley, A. J., & Lipton, A. P. (2004). Immunomodulatory potential of marine secondary metabolites against bacterial diseases of shrimp. *Aquaculture, 230*, 241–248.

Sob, S. V. T., Tane, P., Ngadjui, B. T., Connolly, J. D., & Ma, D. (2007). Trypanocidal labdane diterpenoids from the seeds of *Aframomum aulacocarpos* (Zingiberaceae). *Tetrahedron, 63*, 8993–8998.

Tanaka, R., Ohtsu, H., Iwamoto, M., Minami, T., Tokuda, H., Nishino, H., et al. (2000). Cancer chemopreventive agents, labdane diterpenoids from the stem bark of *Thuja standishii* (Gord.) Carr. *Cancer Letters, 161*, 165–170.